X-ray Binary Luminosity Function Scaling Relations for Local Galaxies Based on Subgalactic Modeling

[Based on Lehmer et al. 2019, ApJS, 243, 3]

SFR

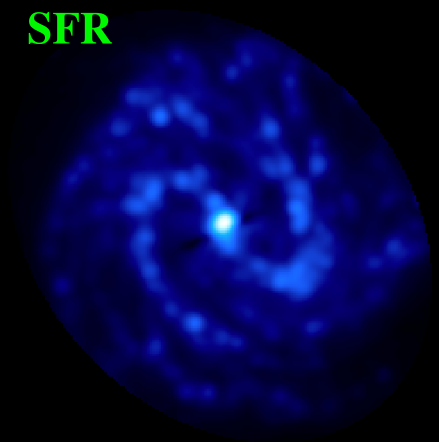

Stellar Mass ($M_\star$)

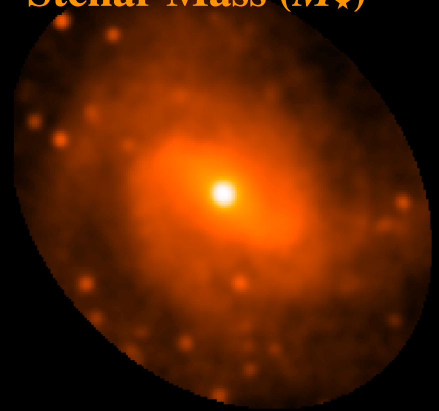

sSFR (SFR/$M_\star$)

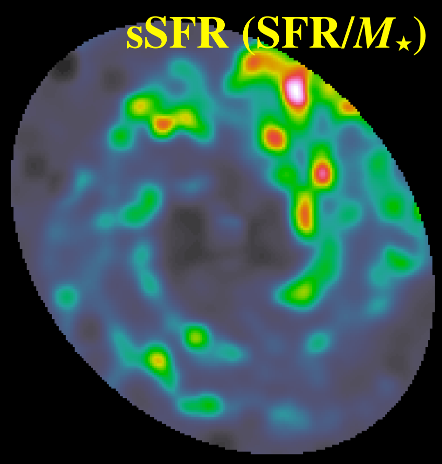

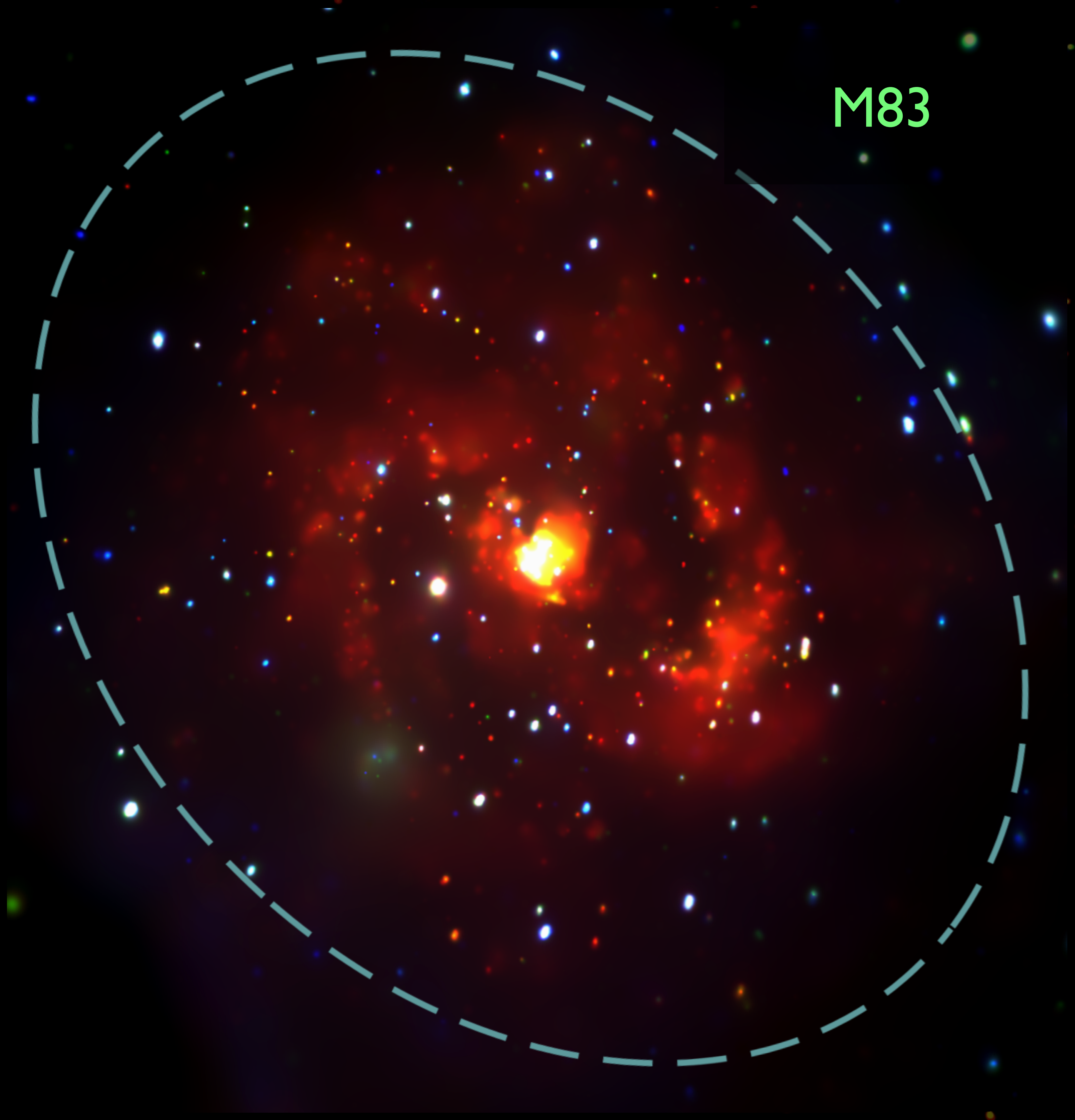

Bret Lehmer

UNIVERSITY OF ARKANSAS

Rafael Eufrasio, Panayiotis Tzanavaris, Antara Basu-Zych, Tassos Fragos, Andrea Prestwich, Mihoko Yukita, Andreas Zezas, Ann Hornschemeier, & Andy Ptak

cf. Talks by Zezas, Fornasini, and Svoboda

XRB Population Constraints from Local Galaxy Samples

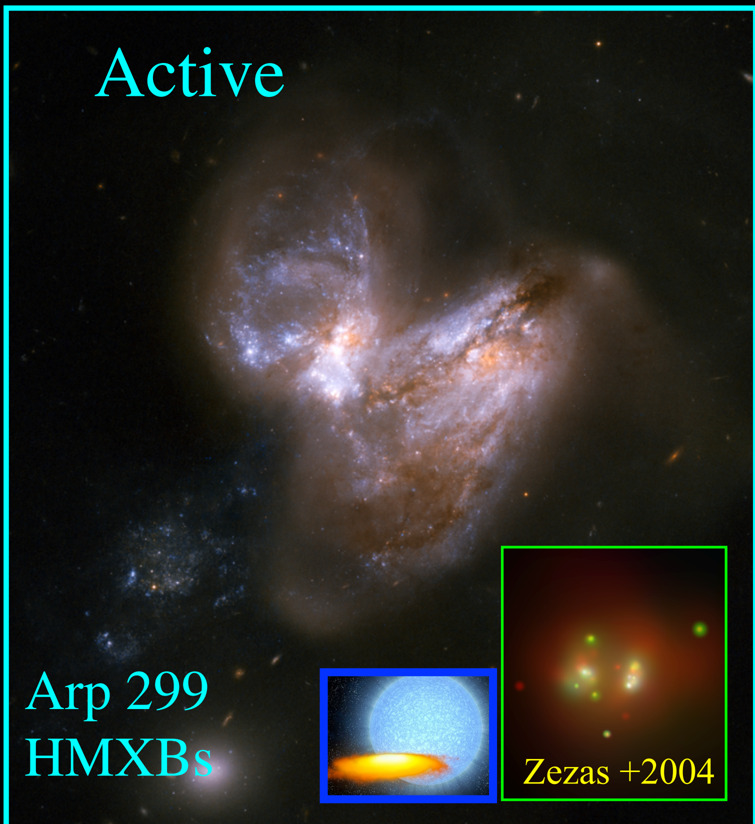

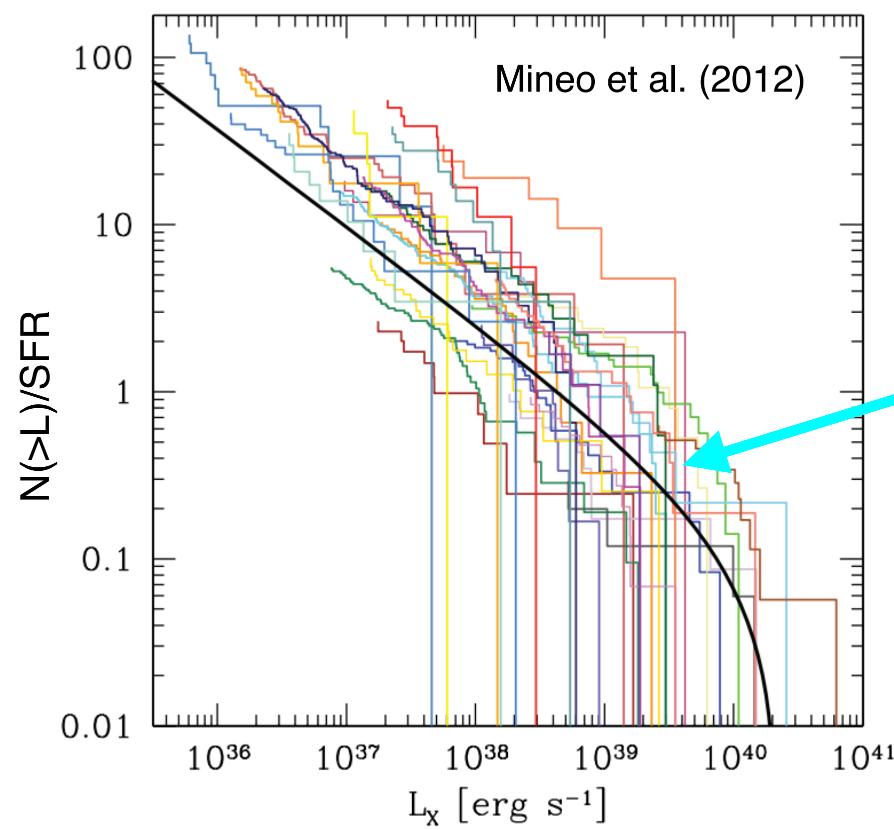

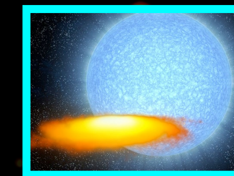

HMXB XLF

Shallow sloped, single power-law with normalization that scales with SFR.

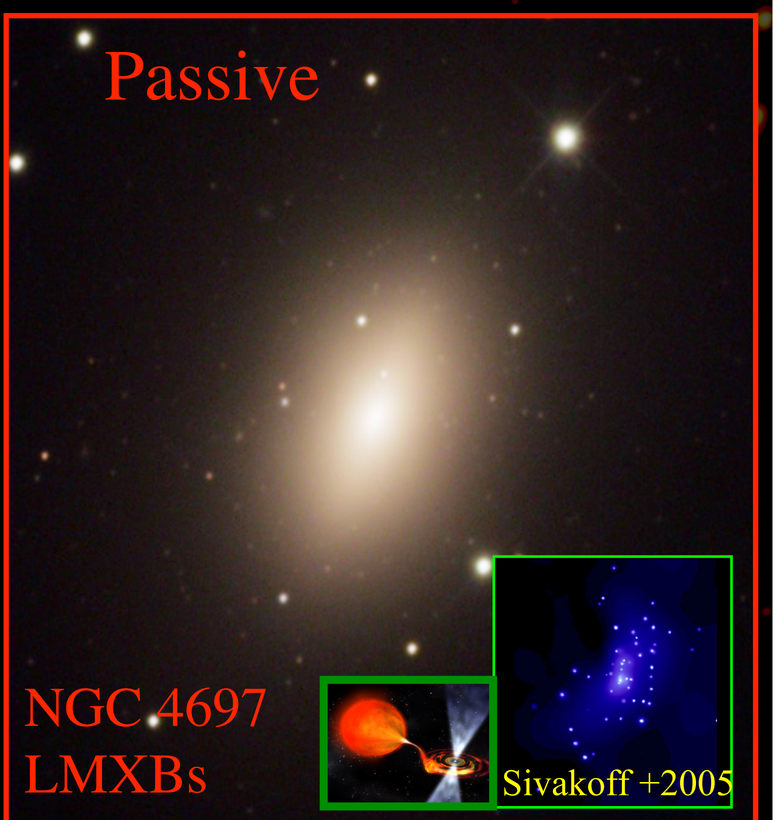

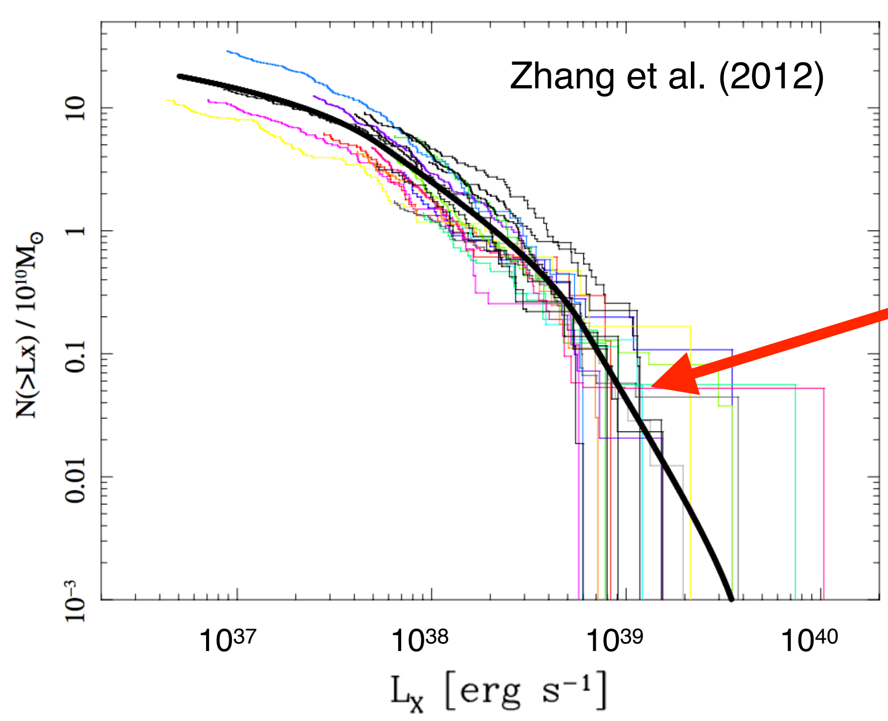

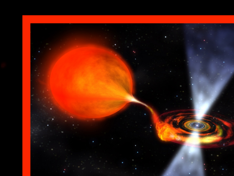

LMXB XLF

Steep-sloped, broken power-law with normalization that scales with $M_\star$.

X-ray Evolution of XRBs From the Chandra Deep Fields

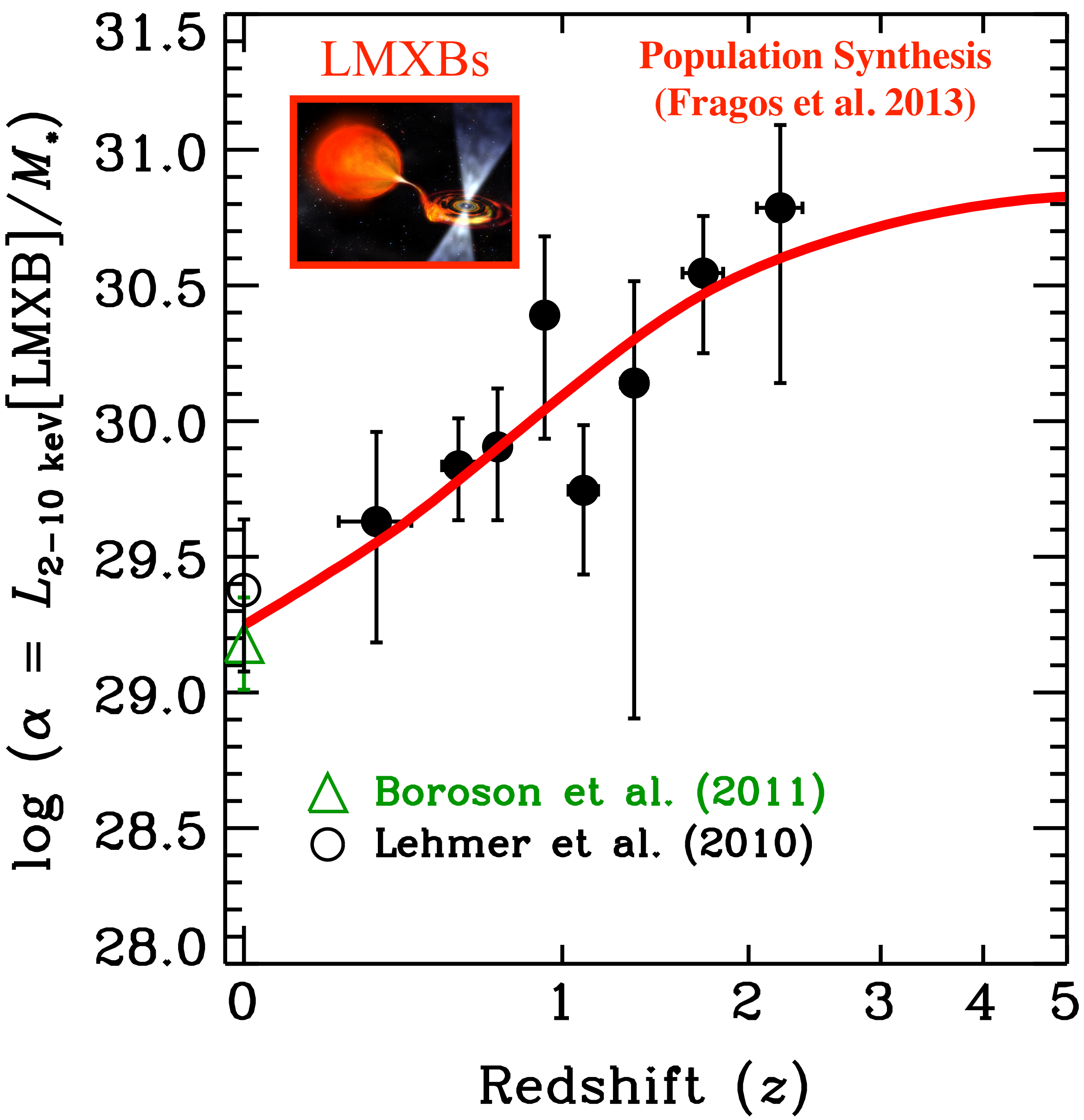

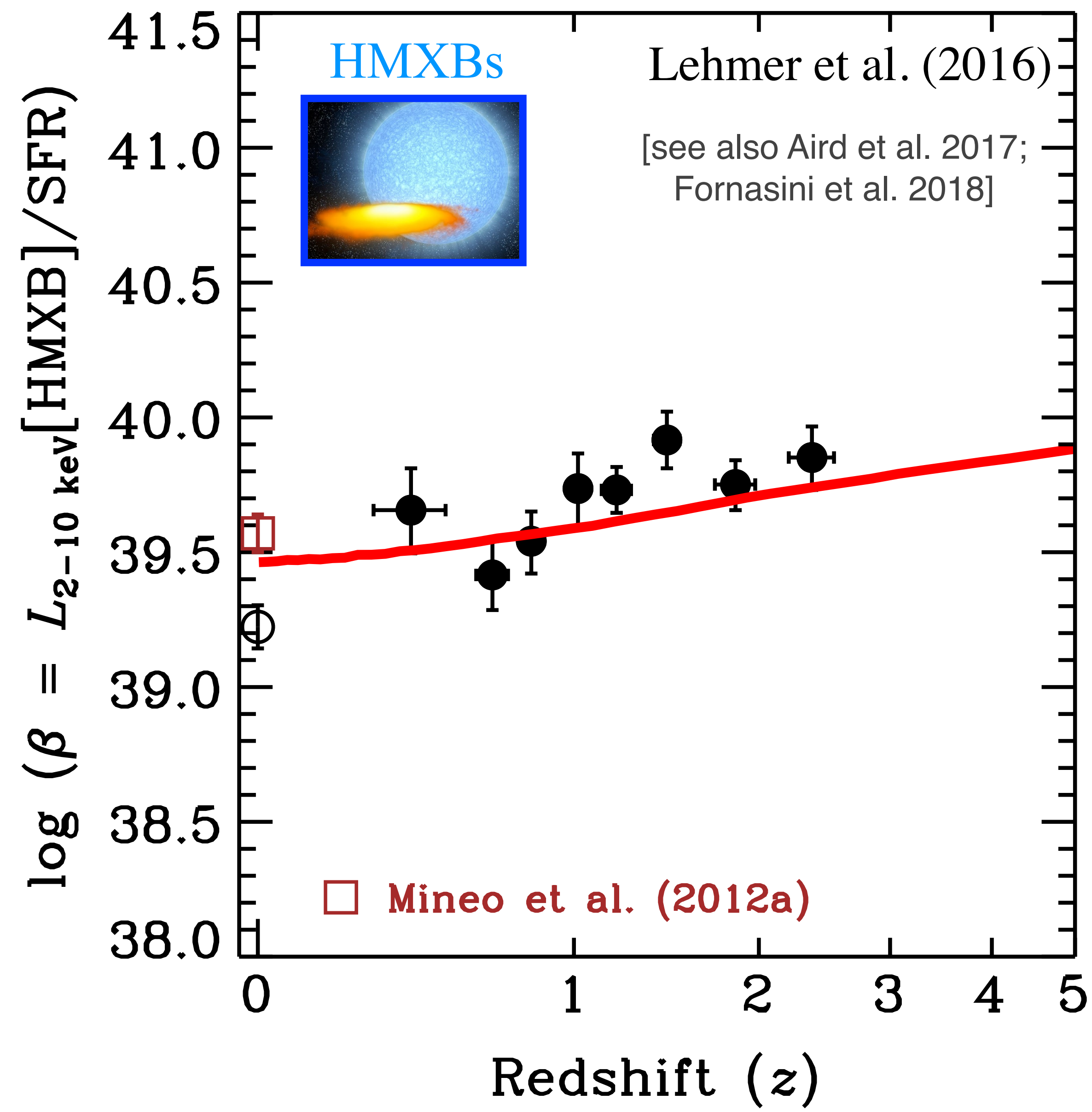

- Younger stellar populations
- More massive donor stars and higher accretion rates
- More luminous LMXBs

- Lower metallicity populations
- Weaker radiative mass losses lead to less binary widening, more massive compact objects, and longer timescales for luminous accretion.
- More luminous HMXBs

Metallicity-Dependence from Local Galaxy Studies

- Correlation studies of local galaxy samples show that L_X/SFR declines with gas-phase metallicity, similar to population synthesis predictions (e.g., Brorby et al. 2016).
- Low metallicity galaxies appear to have an excess of very luminous (>10^{40} erg/s) ULXs in ~0.3 $Z_\odot$ galaxies, but results suffer from confusion and lack of constraints for typical XRBs.

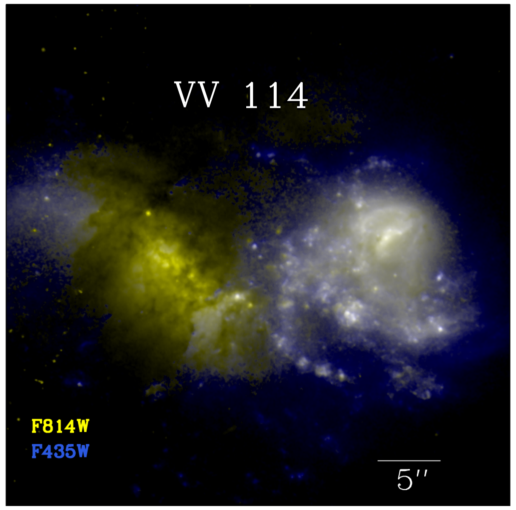

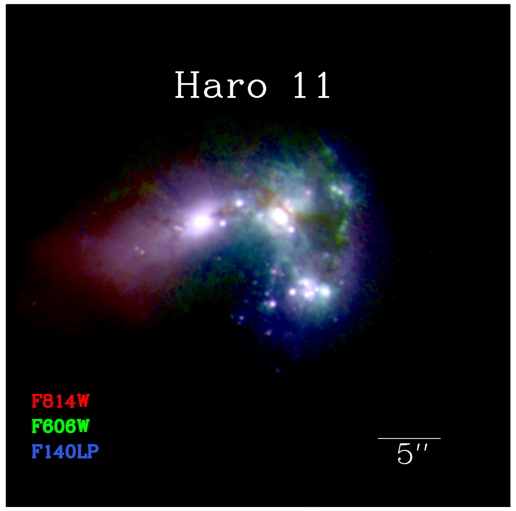

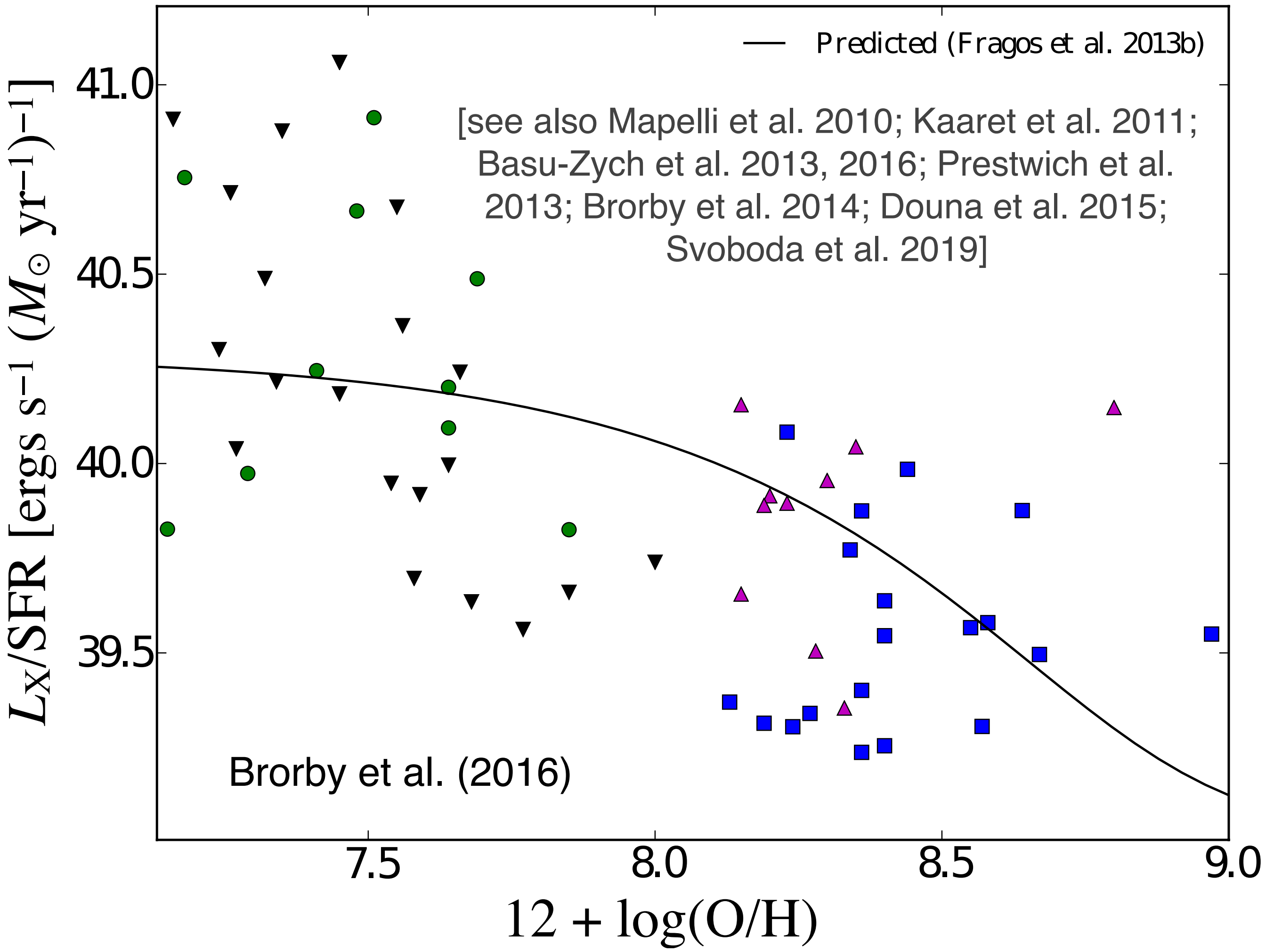

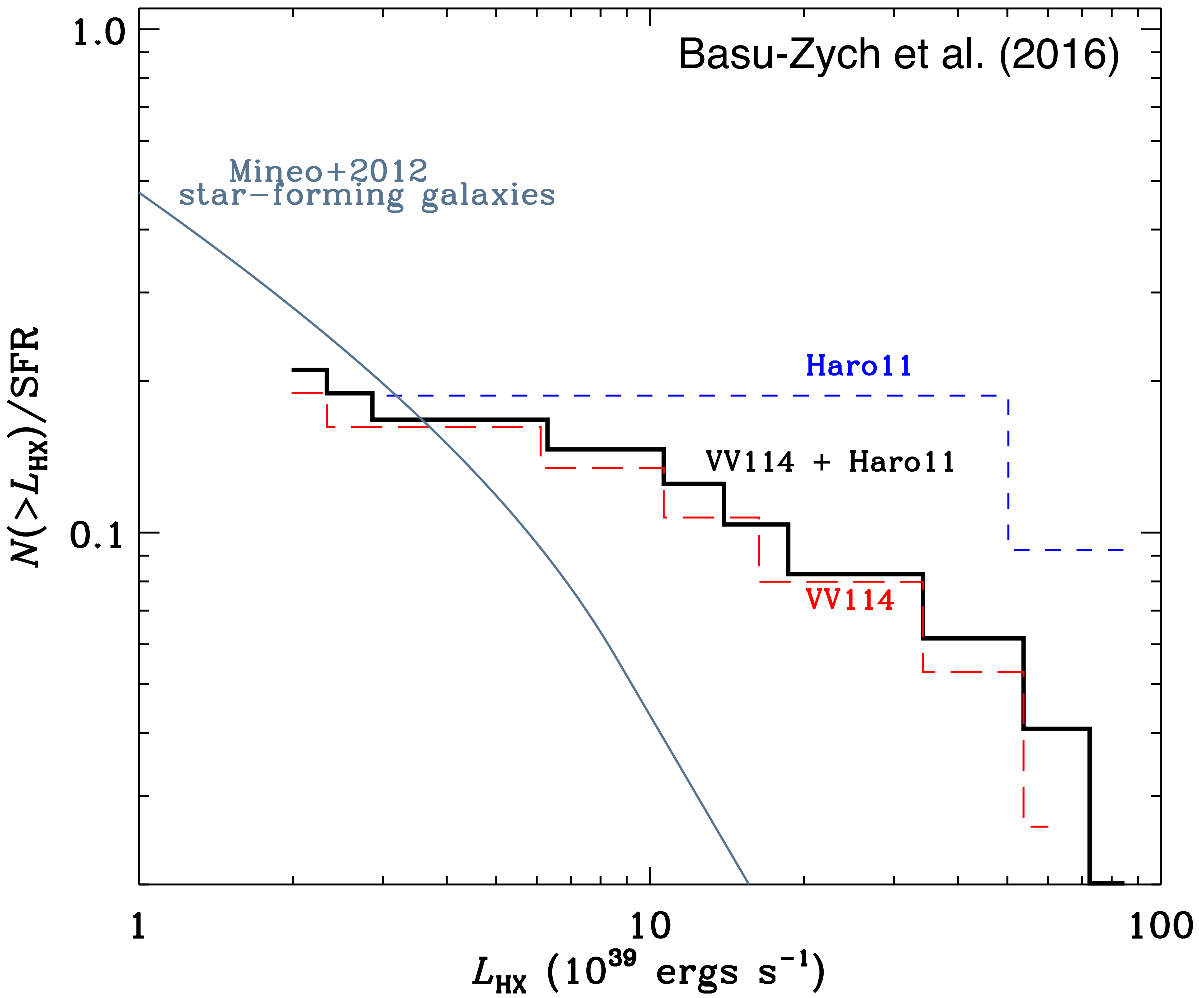

Goal: Extract empirical constraints on how XRB X-ray luminosity functions vary with population age, metallicity, and dynamical environment?

Local Galaxy Sample (Lehmer et al. 2019)

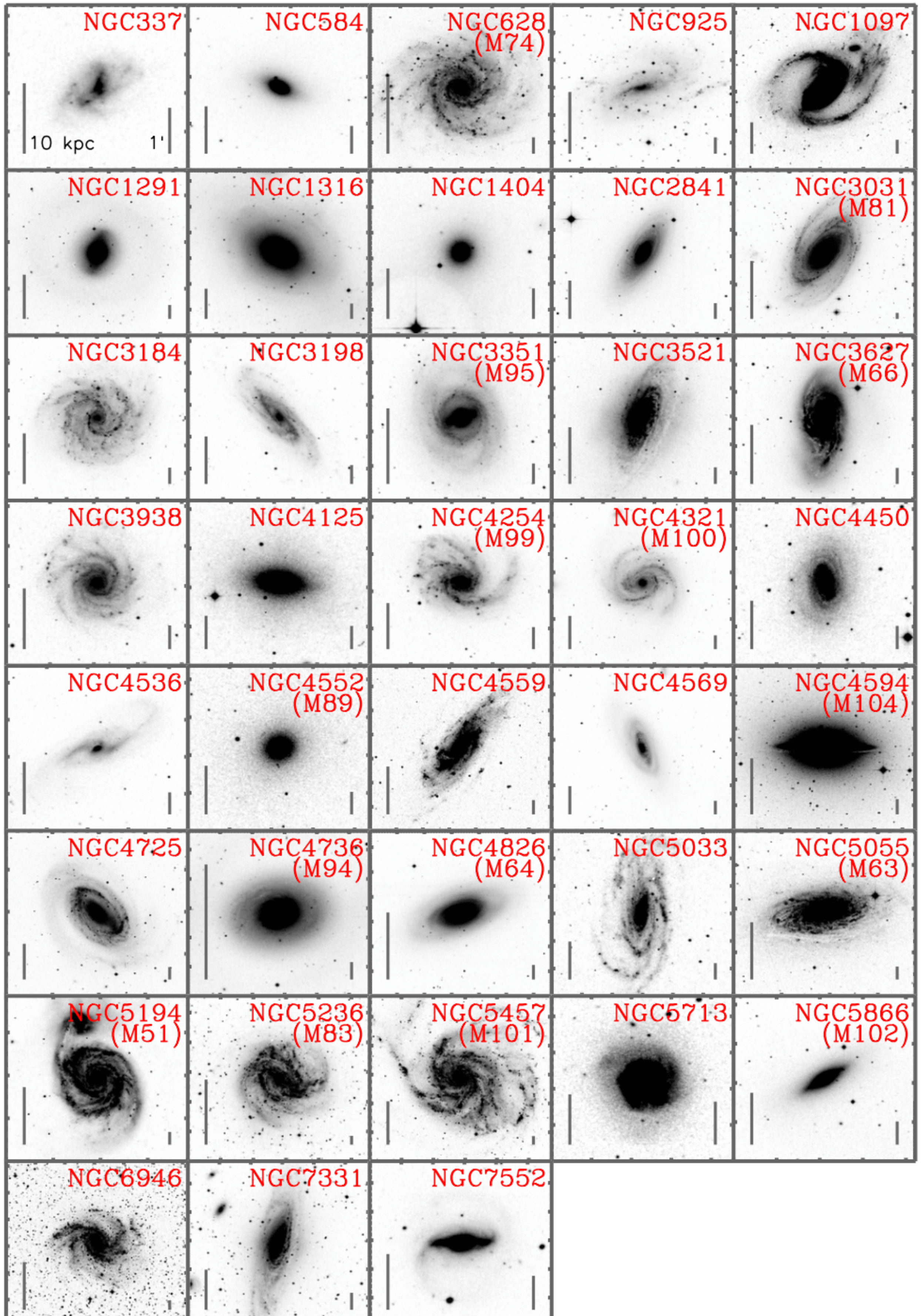

- Select sample of 38 galaxies, mainly from *Spitzer* Infrared Nearby Galaxies Survey (SINGS; Kennicutt et al. 2003):
  - $D < 30$ Mpc (resolve X-ray sources)
  - $M_B < -19$ mag (bright with lots of XRBs)
  - *Chandra* ACIS imaging data (identify XRBs)
  - UV−to−Far-IR data available (local stellar mass, SFR, and sSFR)
- Span broad range of morphology (E to SAc).
- At the subgalactic level (500×500 pc^2 regions), we have a diversity of environments, at log SFR/$M_\star$ (sSFR) = −12.2 to −8.7 [yr^{-1}].
- Have estimates of gas-phase metallicity, mainly from spectroscopy (Moustakas et al. 2010) with $Z = 0.5-1.5\ Z_\odot$.
- Within the galaxy footprints, we have **2478** X-ray sources, and estimate **~540** unrelated cosmic X-ray background objects (Kim et al. 2007).

Extracting Subgalactic X-ray Luminosity Functions

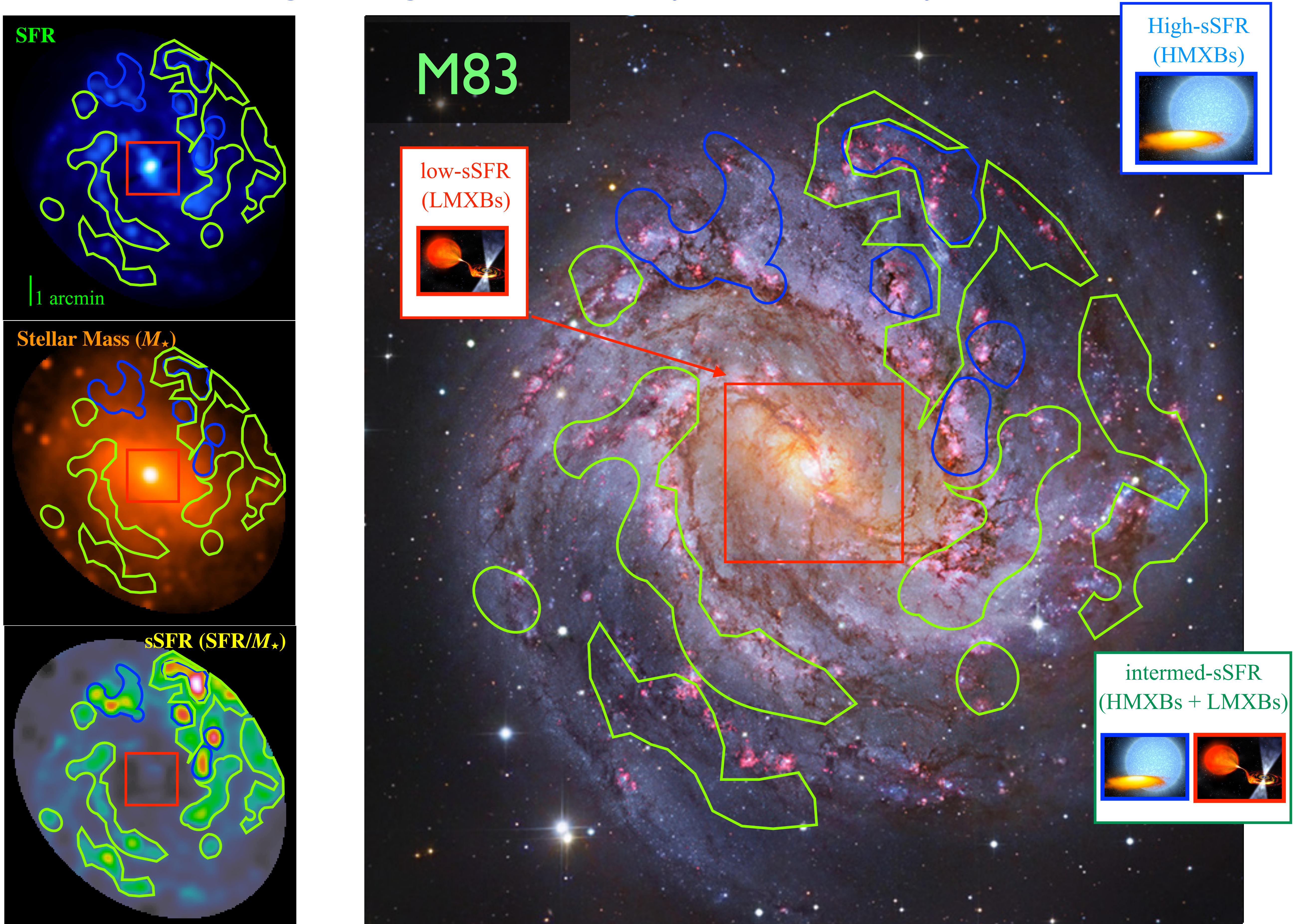

Specific-SFR Dependent X-ray Luminosity Function

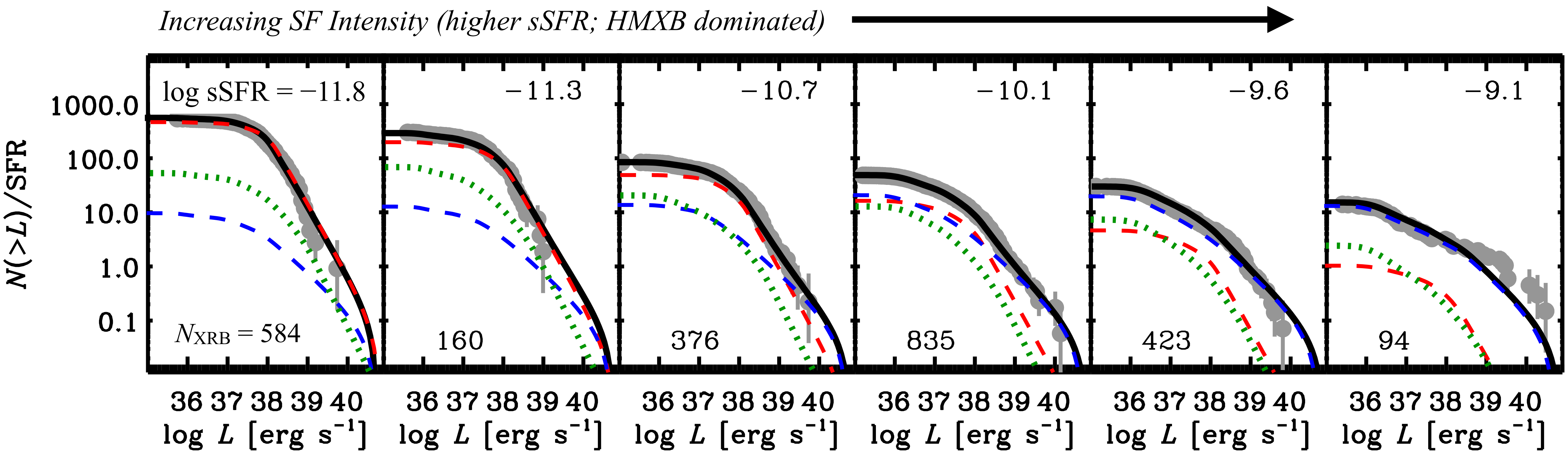

$$\frac{dN}{dL_X} = \xi(L_X)\left[\frac{dN(\mathrm{LMXB})}{dL_X} + \frac{dN(\mathrm{HMXB})}{dL_X} + \mathrm{CXB}\right]$$

$$\frac{dN(\mathrm{HMXB})}{dL_X} = \mathrm{SFR}\, K_{\mathrm{HMXB}} \begin{cases} L_X^{-\gamma} & (L_X < L_c) \\ 0, & (L_X \geq L_c) \end{cases}$$

$$\frac{dN(\mathrm{LMXB})}{dL_X} = M_\star K_{\mathrm{LMXB}} \begin{cases} L_X^{-\alpha_1} & (L_X < L_b) \\ L_b^{\alpha_2-\alpha_1} L_X^{-\alpha_2}, & (L_b \leq L_X < L_c) \\ 0, & (L_X \geq L_c) \end{cases}$$

HMXBs

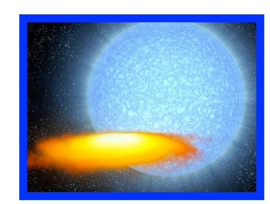

LMXBs

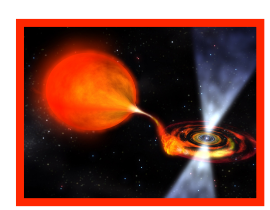

- All seven parameters are well constrained with:

$$K_{\mathrm{HMXB}} = 1.96 \pm 0.14\ (\mathrm{M}_\odot\ \mathrm{yr}^{-1})^{-1}$$

$$\gamma = 1.65^{+0.03}_{-0.02}$$

$$\log L_c = 40.7^{+0.4}_{-0.2}$$

$$K_{\mathrm{LMXB}} = 33.8^{+7.3}_{-3.6}\ (10^{11}\ \mathrm{M}_\odot)^{-1}$$

$$\alpha_1 = 1.28^{+0.06}_{-0.09}$$

$$L_b = 1.48^{+0.70}_{-0.66}\ (10^{38}\ \mathrm{erg\ s}^{-1})$$

$$\alpha_2 = 2.33^{+0.27}_{-0.21}$$

LMXB and HMXB XLFs Detailed

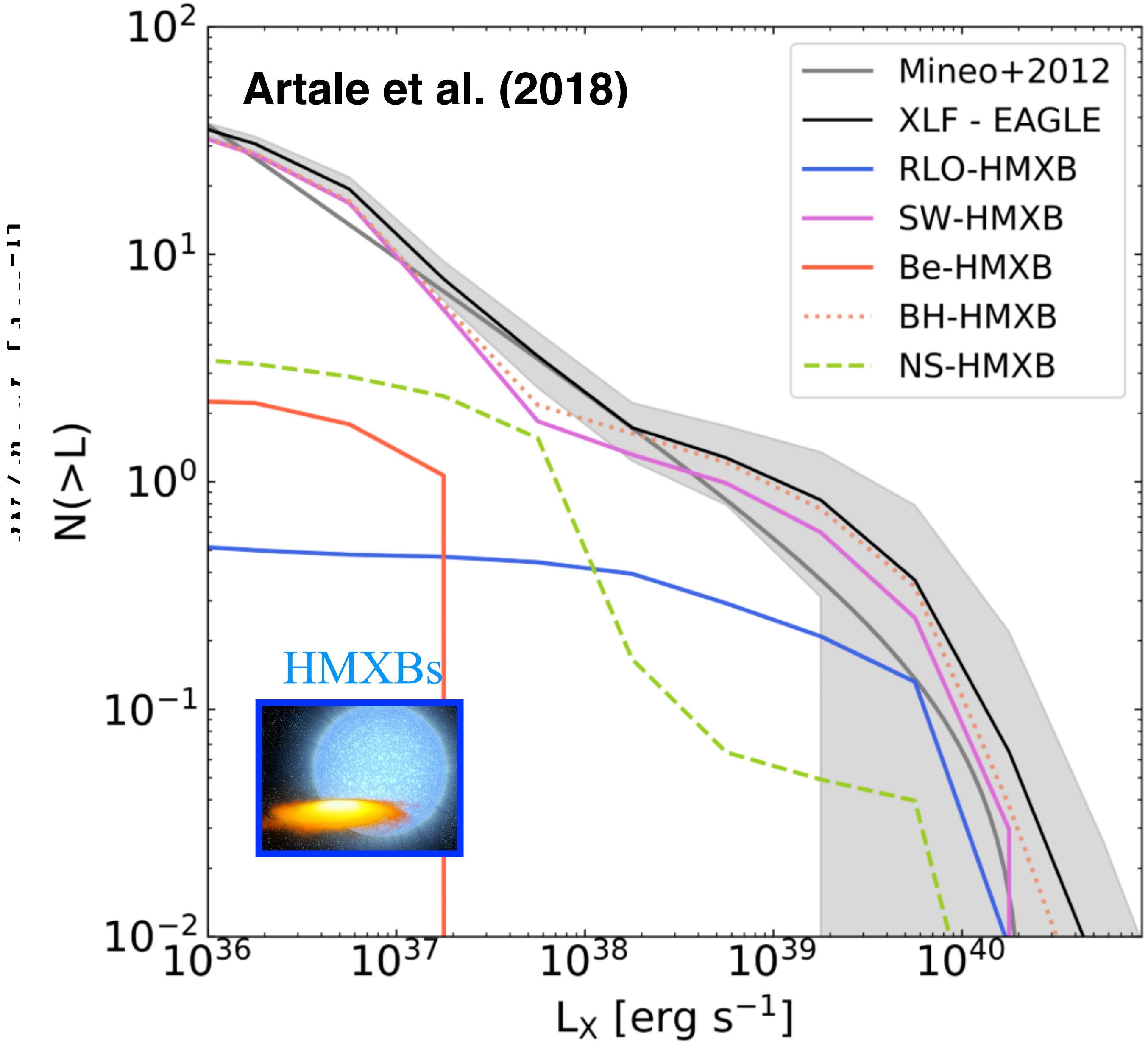

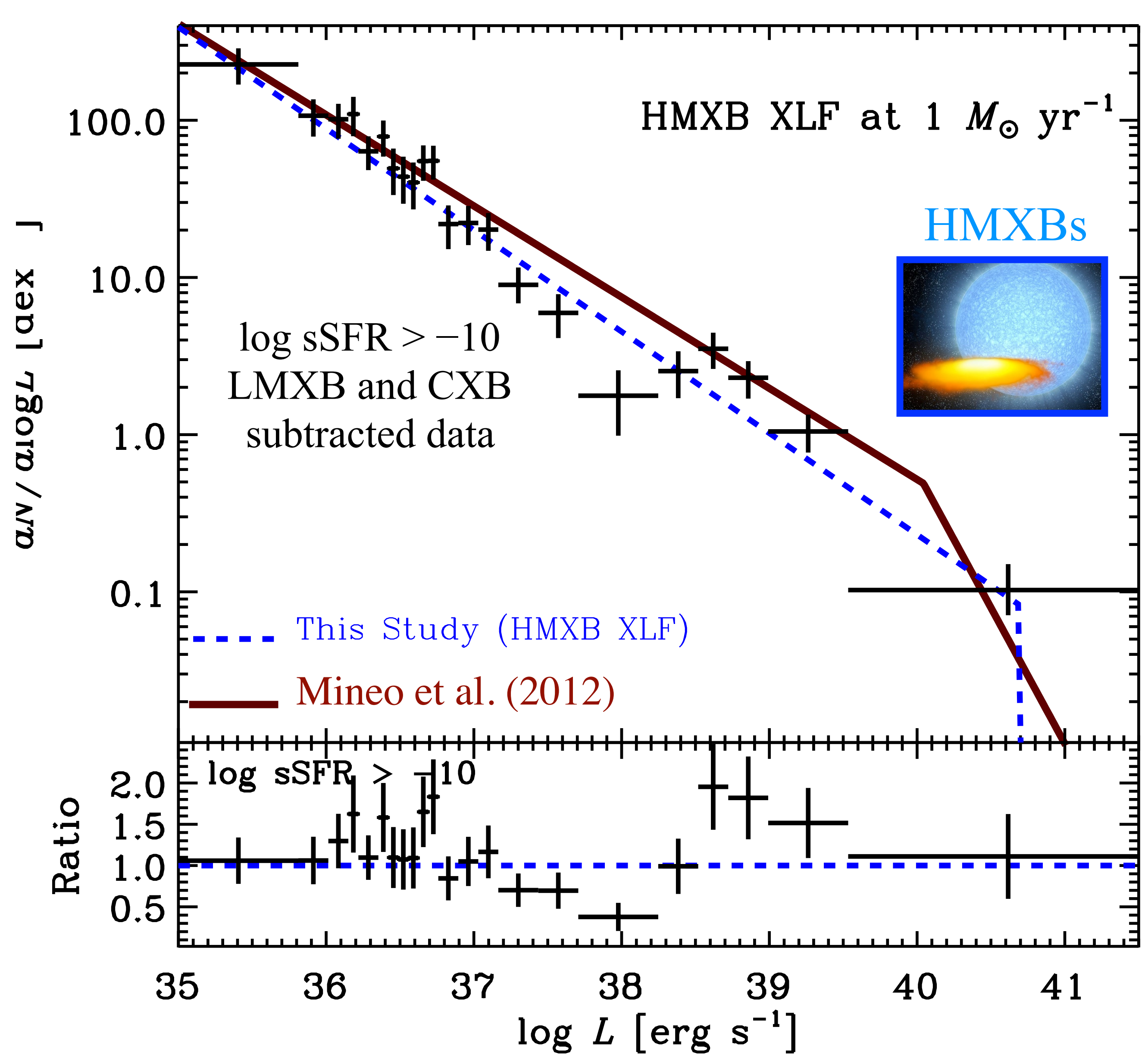

• The LMXB XLF in late-types is somewhat below that derived from Zhang et al. (2012) for elliptical galaxies, potentially due to differences in GC LMXB populations and star-formation histories.

• The HMXB XLF is similar to the Mineo et al. (2012) XLF; however, we identify a more complex shape that should have implications for population synthesis models.

Galaxy-by-Galaxy X-ray Luminosity Functions

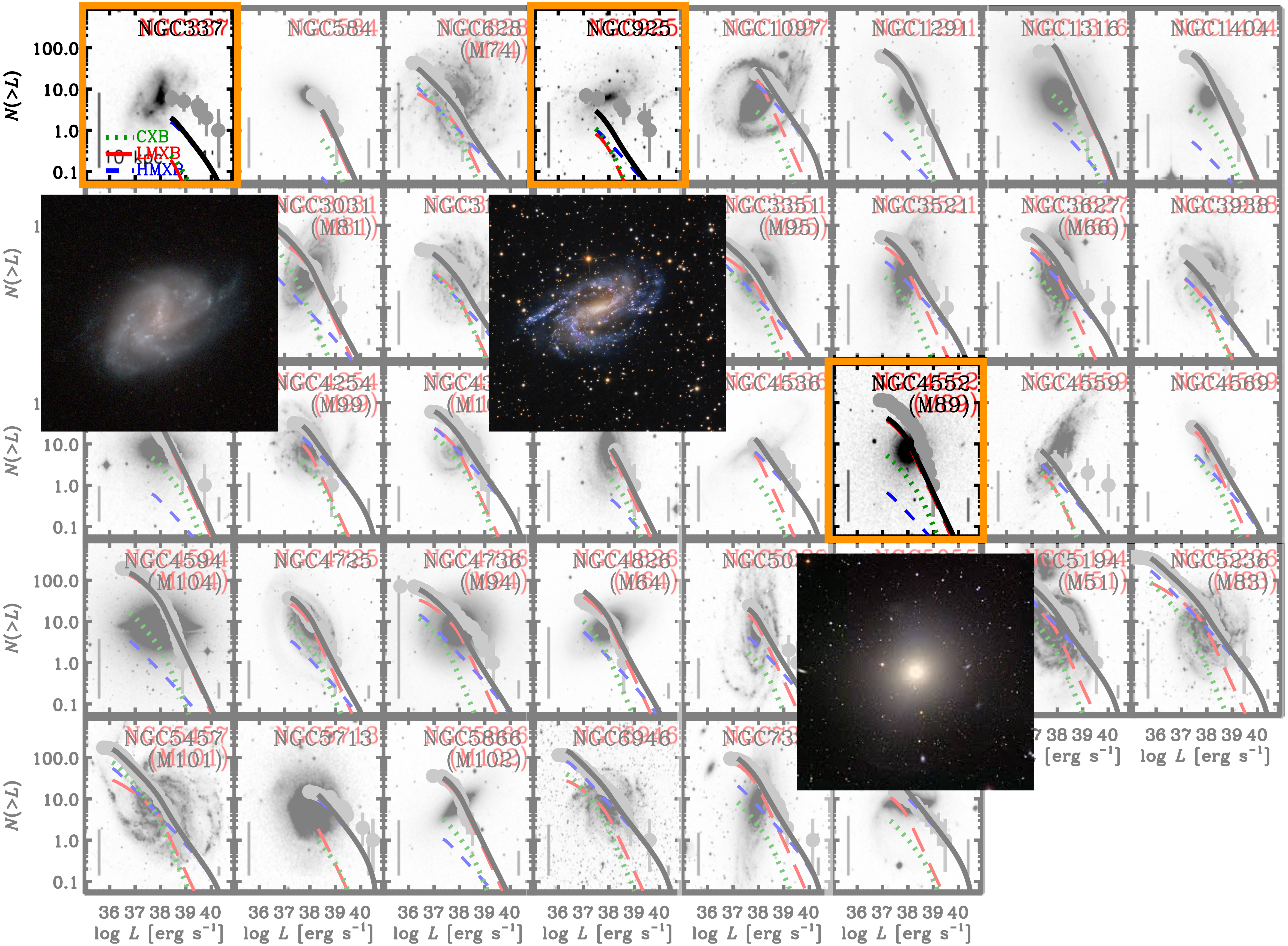

Evidence for a Metallicity Dependence

The average galaxy gas-phase metallicity is ~$Z_\odot$. We identified a subset of four ~$0.5Z_\odot$ galaxies in the sample and inspected their XLFs.

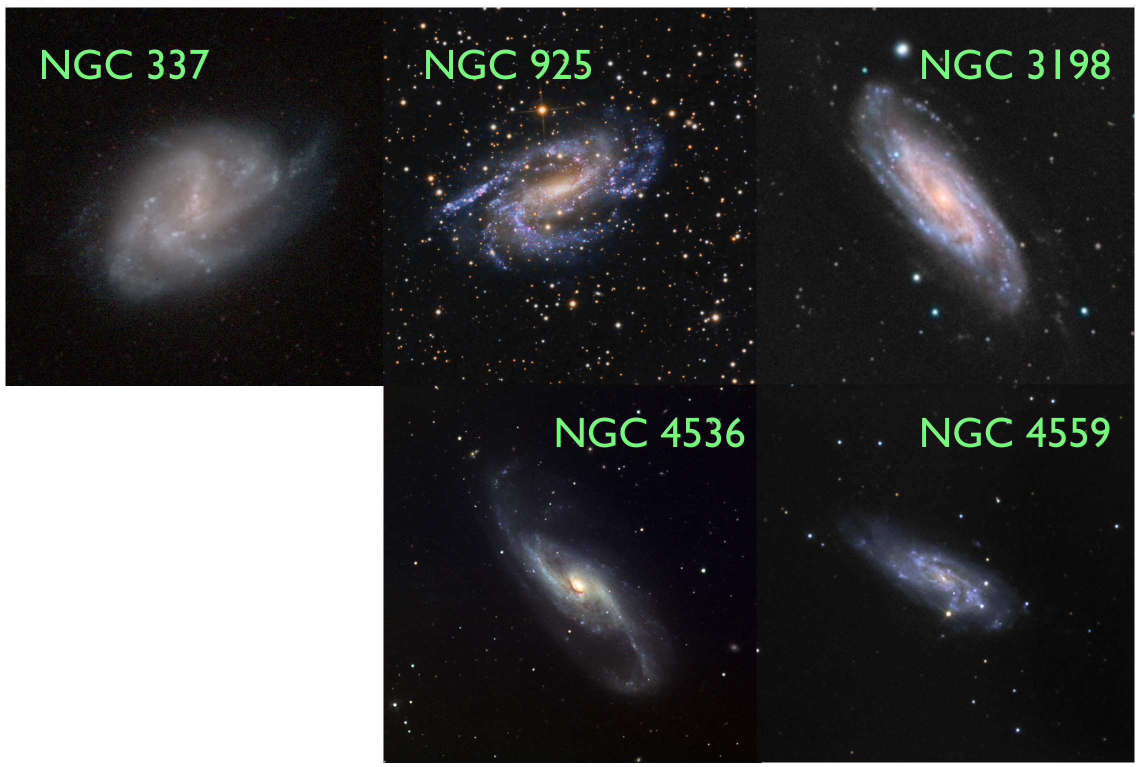

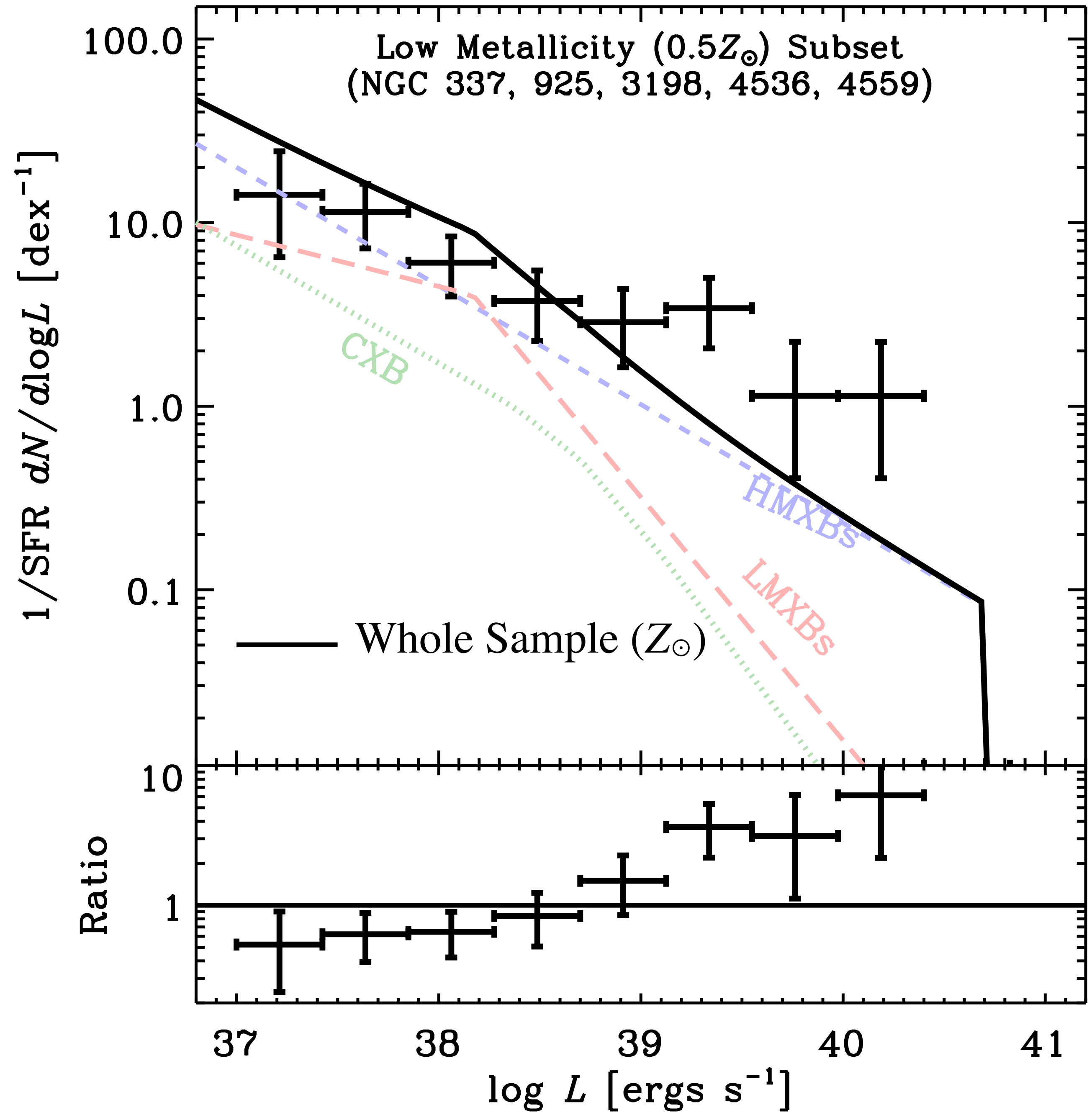

Low-metallicity XLF has factor of ~3−10 times excess of $L > 10^{39}$ ergs s^{-1} sources and potential deficit of lower-luminosity objects. This is overall consistent with L_X/SFR varying with metallicity. Future work is planned to explore the detailed variations in the XLF with metallicity.

Summary and Future Work

1. Self-consistently modeled the HMXB and LMXB populations in subgalactic regions from a sample of 38 galaxies (mainly late-types) and decomposed the HMXB and LMXB XLFs and parameterized their shapes.

2. The LMXB XLF in our sample has a relatively shallow high-L ($>10^{38}$ ergs/s) slope and fewer $L < 10^{38}$ ergs/s sources compared to large ellipticals. This is likely due to differences in GC LMXB populations and younger star-formation histories.

3. The HMXB XLF is basically consistent with previous studies; however, we identify a more complex shape that should have implications for population synthesis models.

4. We find low-metallicity galaxies are outliers to our global parameterization, and contain an excess of ULXs ($L > 10^{39}$ ergs/s) and potentially a deficit of $L \approx 10^{37}-10^{38}$ ergs/s sources.

5. Our results have implications for quantifying the scatter in integrated emission scaling relations (e.g., L_X vs. SFR relation), constraining detailed population synthesis models, quantifying XRB populations when studying AGN, and predicting future mission (e.g., *eROSITA* and *Athena*) X-ray detections of normal galaxies (see Lehmer et al. 2019).

Future Direction

• Long-term goal would be to carefully quantify empirically how the generalized XRB XLFs vary with star-formation history and metallicity using as many relevant data sets as possible.

• Data from such efforts could then be used as a critical set of constraints on stellar population evolution models that include the effects of mass-transfer on binaries (e.g., BPASS; Eldridge et al. 2017) and help put into context interacting binary phenomena like gravitational wave sources.

Best-Fit XLF Parameter Constraints

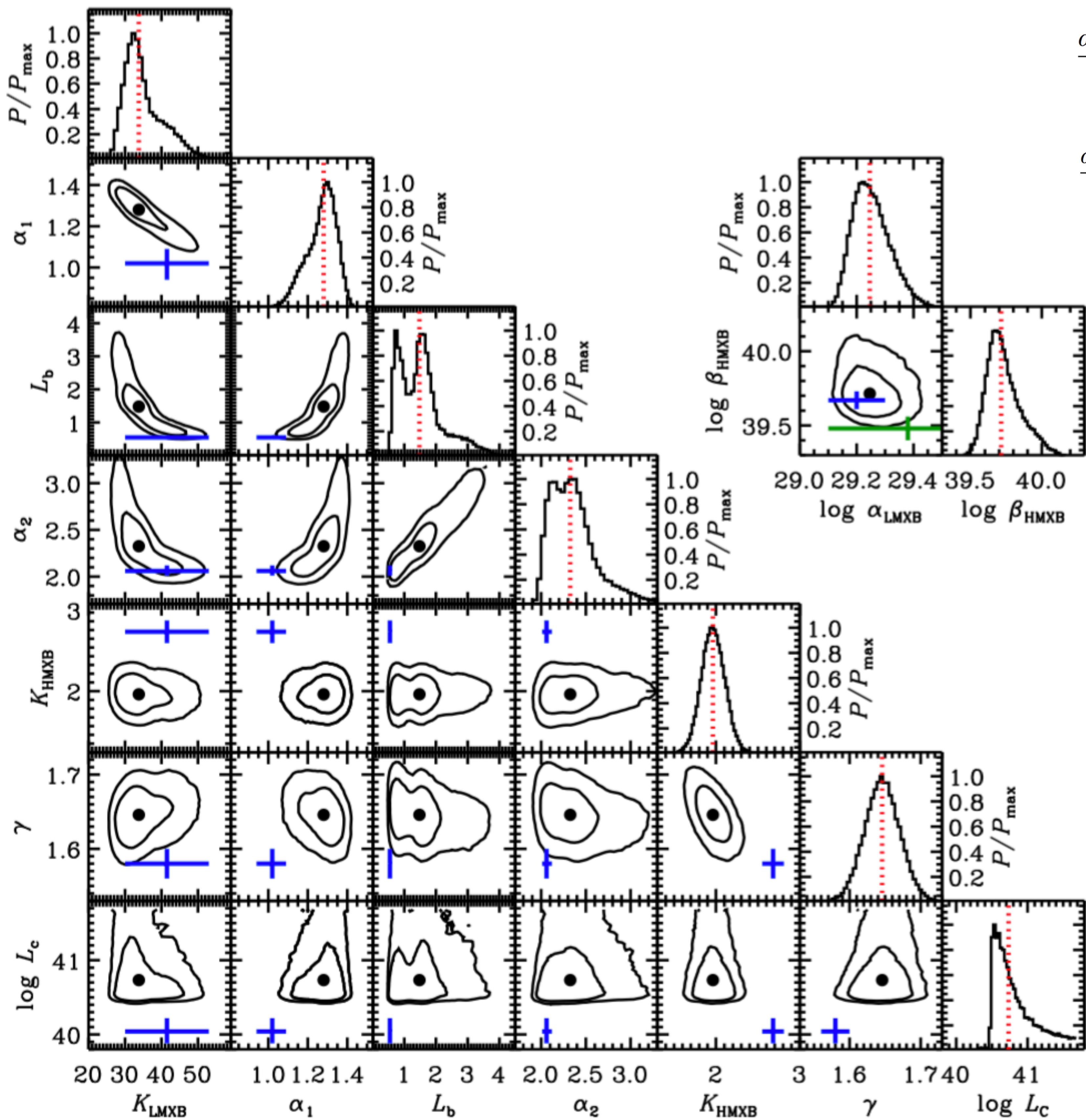

$$\frac{dN(\mathrm{HMXB})}{dL_{\mathrm{X}}} = \mathrm{SFR}\ K_{\mathrm{HMXB}} \begin{cases} L_{\mathrm{X}}^{-\gamma} & (L_{\mathrm{X}} < L_c) \\ 0, & (L_{\mathrm{X}} \geq L_c) \end{cases}$$

$$\frac{dN(\mathrm{LMXB})}{dL_{\mathrm{X}}} = M_\star\ K_{\mathrm{LMXB}} \begin{cases} L_{\mathrm{X}}^{-\alpha_1} & (L_{\mathrm{X}} < L_b) \\ L_b^{\alpha_2-\alpha_1} L_{\mathrm{X}}^{-\alpha_2}, & (L_b \leq L_{\mathrm{X}} < L_c) \\ 0, & (L_{\mathrm{X}} \geq L_c) \end{cases}$$